Polarity effects in the x-ray photoemission of ZnO and other wurtzite semiconductors

M. W. Allen[*] D. Y. Zemlyanov[†] G. I. N. Waterhouse[‡]
J. B. Metson[**] T. D. Veal[††]
C. F. McConville[‡‡] S. M. Durbin[§]

[*]
[†]
[‡]
[**]
[††]
[‡‡]
[§]

Polarity effects in the x-ray photoemission of ZnO and other wurtzite semiconductors

M. W. Allen,[1,6,a)] D. Y. Zemlyanov,[2] G. I. N. Waterhouse,[3,6] J. B. Metson,[3,6] T. D. Veal,[4] C. F. McConville,[4] and S. M. Durbin[5,6]

[1]*Department of Electrical and Computer Engineering, University of Canterbury, Christchurch 8140, New Zealand*
[2]*Birck Nanotechnology Center, Purdue University, West Lafayette, Indiana 47907-2057, USA*
[3]*Department of Chemistry, University of Auckland, Private Bag 90219, Auckland, New Zealand*
[4]*Department of Physics, University of Warwick, Coventry CV4 7AL, United Kingdom*
[5]*Department of Electrical Engineering and Department of Physics, University at Buffalo, Buffalo, New York 14260, USA*
[6]*The MacDiarmid Institute for Advanced Materials and Nanotechnology, New Zealand*

(Received 21 January 2011; accepted 15 February 2011; published online 9 March 2011)

Significant polarity-related effects were observed in the near-surface atomic composition and valence band electronic structure of ZnO single crystals, investigated by x-ray photoemission spectroscopy using both Al K_α (1486.6 eV) and synchrotron radiation (150 to 1486 eV). In particular, photoemission from the lowest binding energy valence band states was found to be significantly more intense on the Zn-polar face compared to the O-polar face. This is a consistent effect that can be used as a simple, nondestructive indicator of crystallographic polarity in ZnO and other wurtzite semiconductors. © *2011 American Institute of Physics*. [doi:10.1063/1.3562308]

ZnO is a candidate for next-generation optoelectronic devices due to a unique combination of properties, including a wide direct band gap in the ultraviolet-A spectrum, efficient above room temperature free-excitonic emission, and large spontaneous and piezoelectric polarizations.[1] However, many of the optical and electrical properties of ZnO, including photoluminescence,[2] cathodoluminescence,[3] near-surface electron accumulation,[4] and the barrier heights of Schottky contacts[5] vary with crystallographic polarity. Polarity also plays an important role in ZnO growth, affecting surface morphology, crystal quality, and dopant incorporation.[6] Existing methods for determining the polarity of ZnO surfaces, which include wet etching,[7] coaxial impact-collision ion scattering spectroscopy,[8] and x-ray diffraction,[9] are time consuming and difficult to perform *in situ* during film growth and device fabrication.

X-ray photoemission spectroscopy (XPS) is a widely used tool for probing the chemical and electronic nature of semiconductor surfaces, with *in situ* XPS increasingly used during the growth of epitaxial films and heterostructures. In this letter, we report significant polarity-related differences in the XPS spectra of ZnO and other wurtzite semiconductors which provide a simple nondestructive indicator of crystallographic polarity.

ZnO crystallizes into the wurtzite structure which when viewed along the *c*-axis (Fig. 1) consists of alternating planes of Zn and O atoms, arranged in threefold coordinated "double layers" separated by a single Zn–O bond. Truncation of the crystal along this axis always results in one of two polar surfaces—the Zn-polar [ZnO(0001)Zn] face or the O-polar [ZnO(000$\bar{1}$)O] face. Due to the large electronegativity of oxygen, these polar faces have a significant ionic character and are electrostatically unstable.[10,11] Three stabilization mechanisms are commonly proposed: (a) a fractional negative charge transfer from the O-polar to Zn-polar face, (b) a surface reconstruction which removes 25% of the surface atoms, and (c) the adsorption of hydroxide [hydrogen] on the Zn-polar [O-polar] face.[10–13] In the case of the Zn-polar face, some form of condition-dependent (i.e., *p*H, temperature, H_2/H_2O partial pressure) competition between the formation of triangular islands and pits with O-terminated step edges and the adsorption of hydroxyl (OH) groups may occur.[12,13] The O-polar face, except under rare circumstances, has been shown to exhibit an unreconstructed (1×1) H-termination.[14,15]

Polarity-related differences in the XPS spectra of ZnO were investigated using *c*-axis, *m*-plane $(1\bar{1}00)$, and *a*-plane $(11\bar{2}0)$ bulk ZnO single crystal wafers $(10\times10\times0.5\ \text{mm}^3)$ grown using both the hydrothermal (HT) and pressurized-melt (PM) techniques.[6,16] The carrier concentration of the HT and PM ZnO material was 10^{13}–10^{14} cm^{-3} and 10^{16}–10^{17} cm^{-3}, respectively, allowing the influence of bulk conductivity to also be investigated. Zn-polar and O-polar face samples were cut from the same double-sided polished *c*-axis wafers. All samples were ultrasonically cleaned using

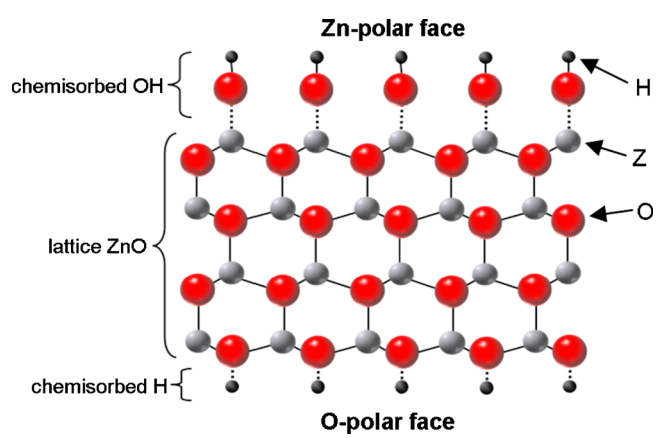

FIG. 1. (Color online) The Zn-polar (0001) and O-polar (000$\bar{1}$) hydroxyl-terminated faces of wurtzite ZnO.

[a)]Electronic mail: martin.allen@canterbury.ac.nz.

TABLE I. XPS ($h\nu$=1486.6 eV) quantification analysis of the organic-solvent cleaned Zn-polar, O-polar, and *m*-plane faces of HT ZnO before and after 20 min ROP exposure.

Preparation	Sample	Atomic composition (%)			
		Zn	O	C	Zn/O
Organic solvent cleaned	Zn-polar	34.0	51.4	14.6	0.66
	O-polar	35.7	47.1	17.2	0.75
	m-plane	35.8	45.0	19.3	0.79
Remote oxygen plasma cleaned	Zn-polar	45.2	52.4	2.4	0.86
	O-polar	49.3	47.9	2.8	1.03
	m-plane	49.9	47.5	2.6	1.05

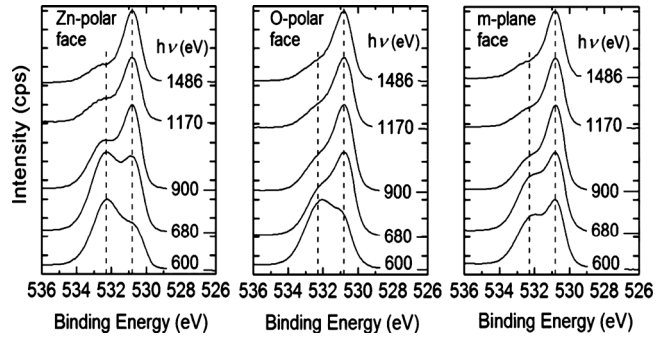

FIG. 2. O 1*s* core-level XPS spectra (pass energy=10 eV) taken at incident photon energies from 1486 to 600 eV on the Zn-polar, O-polar, and *m*-plane faces of organic-solvent cleaned HT ZnO.

organic solvents (acetone, methanol, and isopropyl alcohol) and dried in N_2 gas. XPS measurements were performed using a Kratos Ultra DLD spectrometer and monochromated Al K_α radiation ($h\nu$=1486.6 eV) at Purdue University and at the soft x-ray beamline of the Australian Synchrotron using photon energies from 150 to 1486 eV. Unless otherwise stated, the spectra were collected with the detector axis normal to the sample surface (take-off angle θ=90°). Monochromated Al K_α XPS measurements were also carried out on additional samples using a Kratos XSAM800 spectrometer at the University of Auckland and a Scienta ESCA 300 spectrometer at the National Centre for Electron Spectroscopy and Surface Analysis, Daresbury Laboratory U.K., to confirm the reproducibility of the polarity-related effects. All samples were carefully grounded to the respective spectrometer (including samples with indium back contacts) to avoid peak distortion due to sample charging.

We first consider polarity-related differences in the core-level XPS spectra of ZnO: Al K_α XPS survey spectra were taken from the Zn-polar, O-polar, and *m*-plane faces of organic-solvent cleaned HT ZnO. In each case, the survey spectra identified Zn, O, and C as the only elements present in the near-surface region. The atomic concentrations of each element were determined from the areas of the Zn 2*p*, O 1*s*, and C 1*s* core-level peaks using sensitivity factors based on spectrometer-modified Scofield cross-sections. Table I shows the results of this quantification analysis before and after 20 min of remote oxygen plasma (ROP) exposure. Surprisingly, the Zn/O ratio determined for the Zn-polar face was lower than that for the O-polar and *m*-plane faces. This polarity-related effect became even clearer after ROP exposure which drastically decreased the surface carbon contamination and associated O-containing carbonate and carboxyl groups. After ROP exposure, the Zn/O ratios for the O-polar and *m*-plane faces were close to unity, while the ratio for the Zn-polar face was significantly lower. On further investigation, this effect was found to be a consistent phenomenon across multiple HT and PM ZnO wafers.

The origin of the lower Zn/O ratio on the Zn-polar face may be due to a different surface reconstruction and/or the presence of different terminating species compared to the other faces: atomic force microscopy images[5] of the Zn-polar face of HT ZnO revealed the presence of a high density of triangular shaped terraces and pits, similar to those observed by Dulub *et al.*,[10] which are not present on the O-polar or *m*-plane faces. Since the step edges of these features are O-terminated, they lower the effective Zn/O ratio on the Zn-polar face.[10,12]

The termination of the ZnO surface can be determined from the O 1*s* core-level spectra. Figure 2 shows O 1*s* spectra taken at different photon energies (1486 to 600 eV) from organic-solvent cleaned HT ZnO samples at the Australian Synchrotron. The surface sensitivity of the spectra increases with decreasing photon energy, since the inelastic mean free path of the photoemitted electrons is a function of their kinetic energy and approaches a minimum at ~70 eV. For $h\nu$=1486 eV, the dominant emission is at 530.8 eV due to oxygen in the bulk, with a high binding energy shoulder at 532.3 eV associated with the presence of OH groups.[12,14] The intensity of the OH contribution increases significantly with decreasing photon energy indicating that all three faces contain a significant amount of OH bonding localized at the surface. Since the hydroxyl termination at the Zn-polar face is ZnO(0001)Zn–OH compared to ZnO($000\bar{1}$)O–H for the O-polar face,[12–14] hydroxylation of the ZnO surface effectively places additional O atoms at the Zn-polar face, also lowering the Zn/O ratio.

We now consider polarity-related differences in the valence band XPS (VB-XPS) spectra of ZnO: The position of the low binding energy edge of the VB-XPS spectra has previously been used to investigate the near-surface band bending in ZnO.[4] Here, we focus on the shape of the VB-XPS spectra which is closely related to the total valence band density of states.[17] Figure 3(a) shows VB-XPS spectra collected from the Zn-polar, O-polar, and *m*-plane faces of HT ZnO using Al K_α radiation. The VB-XPS spectra consist of two main peaks—peak I at ~5.0 eV which has been attributed to predominately O 2*p* derived states and peak II at ~7 eV which has a hybridized O 2*p*, Zn 4*s*, and (possibly) Zn 3*d* character.[17,18] While the intensity of peak II is similar on all three faces, a striking polarity-related effect involving the intensity of peak I is evident. Peak I is significantly more intense than peak II on the Zn-polar face, while on the O-polar face it is slightly weaker. The intensity of peak I on the nonpolar *m*-plane face is intermediate between that on the two polar faces. The same effect was consistently observed on the Zn-polar, O-polar, and *a*-plane faces of PM ZnO [Fig. 3(c)] and on multiple additional wafers of both types. Interestingly, Ohashi *et al.*[19] also observed a structure, at a similar binding energy to peak I, in the hard ($h\nu$ =5946.8 eV) x-ray VB-XPS spectra of ZnO for only the Zn-polar face.

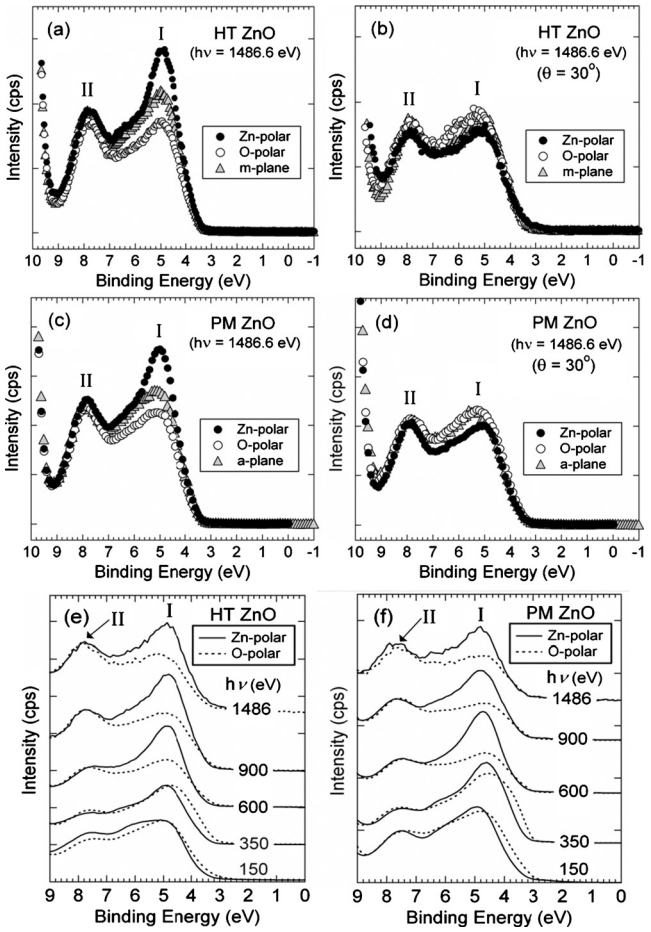

FIG. 3. VB-XPS spectra (pass energy=20 eV) from the polar and nonpolar faces of HT and PM bulk ZnO measured using [(a)–(d)] Al K_α radiation (1486.6 eV) and [(e) and (f)] synchrotron radiation (1486 to 150 eV). The spectra in [(b) and (d)] were collected at a take-off angle $\theta=30°$.

Since peak I has been attributed to mainly O 2*p* derived VB states,[17,18] the increased intensity of this peak on the Zn-polar face could be a surface effect linked to the lower Zn/O ratio and/or the nonhybridized O-orbitals in the OH termination of this face. However, the polarity effect disappears in spectra measured at a take-off angle of $\theta=30°$ to the sample surface [Figs. 3(b) and 4(d)] which represents a two-fold increase in surface sensitivity. This indicates that the polarity effect has a strong directional dependence and may be linked to the lack of inversion symmetry of the wurtzite structure rather than differences in surface reconstruction and chemistry.

The VB-XPS polarity effect was also investigated using synchrotron radiation as shown in Figs. 3(e) and 3(f). The same striking polarity-related difference in the intensity of peak I was observed at photon energies from 1486 to 600 eV, however, at photon energies below 600 eV the difference disappeared. Since the photoemission cross-sections for O 2*p* and Zn 4*s* states are similar in nature over the photon energy range investigated,[20] this also suggests a structural-related cause for the polarity effect. VB-XPS spectra were also taken from the polar faces of double-sided polished *c*-axis CdS and CdSe single crystals. Figures 4(a) and 4(b) show a similar polarity effect for these II–VI wurtzite semiconductors. In addition, Veal *et al.*[21] reported a similar effect in the VB-XPS spectra of InN, which we have also observed in GaN (not shown). This links the polarity effect to the common wurtzite structure rather than to specific differences in the surface chemistry of these semiconductors.

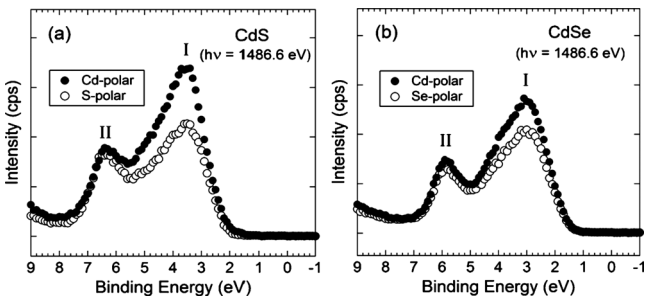

FIG. 4. VB-XPS spectra from the polar faces of (a) CdS and (b) CdSe c-axis single crystals, measured using Al K_α radiation.

In summary, the polar and nonpolar surfaces of ZnO were investigated using XPS. Two significant polarity-related effects were observed in that the Zn/O ratio was consistently lower on the Zn-polar face than on the O-polar and m-plane faces, while photoemission (for $h\nu=1486$ to 600 eV) from the lowest binding energy valence band states was significantly stronger on the Zn-polar face. The latter provides a reliable nondestructive indicator of surface polarity in ZnO which can be used *in situ* during growth and device fabrication.

This work was supported in part by the Marsden Fund (Grant No. UOC0909). We also acknowledge beamtime and the assistance of Dr B. Cowie at the Australian Synchrotron, Victoria, Australia, and the assistance of Dr C. S. Doyle and L. Perander of the University of Auckland.

[1] C. Klingshirn, ChemPhysChem **8**, 782 (2007).
[2] M. W. Allen, P. Miller, R. J. Reeves, and S. M. Durbin, Appl. Phys. Lett. **90**, 062104 (2007).
[3] Y. F. Dong, Z. Q. Fang, D. C. Look, G. Cantwell, J. Zhang, J. J. Song, and L. J. Brillson, Appl. Phys. Lett. **93**, 072111 (2008).
[4] M. W. Allen, C. H. Swartz, T. H. Myers, T. D. Veal, C. F. McConville, and S. M. Durbin, Phys. Rev. B **81**, 075211 (2010).
[5] M. W. Allen, R. J. Mendelsberg, R. J. Reeves, and S. M. Durbin, Appl. Phys. Lett. **94**, 103508 (2009).
[6] E. Ohshima, H. Ogino, I. Niikura, K. Maeda, M. Sato, M. Ito, and T. Fukuda, J. Cryst. Growth **260**, 166 (2004).
[7] A. N. Mariano and R. E. Hanneman, J. Appl. Phys. **34**, 384 (1963).
[8] T. Ohnishi, A. Ohtomo, M. Kawasaki, K. Takahashi, M. Yoshimoto, and H. Koinuma, Appl. Phys. Lett. **72**, 824 (1998).
[9] H. Tampo, P. Fons, A. Yamada, K.-K. Kim, H. Shibata, K. Matsubara, S. Niki, H. Yoshikawa, and H. Kanie, Appl. Phys. Lett. **87**, 141904 (2005).
[10] O. Dulub, U. Diebold, and G. Kresse, Phys. Rev. Lett. **90**, 016102 (2003).
[11] G. Kresse, O. Dulub, and U. Diebold, Phys. Rev. B **68**, 245409 (2003).
[12] A. Önsten, D. Stoltz, P. Palmgren, S. Yu, M. Göthelid, and U. O. Karlsson, J. Phys. Chem. C **114**, 11157 (2010).
[13] M. Valtiner, S. Borodin, and G. Grundmeier, Langmuir **24**, 5350 (2008).
[14] M. Kunat, S. Gil Girol, T. Becker, U. Burghaus, and C. Wöll, Phys. Rev. B **66**, 081402 (2002).
[15] B. Meyer, Phys. Rev. B **69**, 045416 (2004).
[16] J. Nause and B. Nemeth, Semicond. Sci. Technol. **20**, S45 (2005).
[17] P. D. C. King, T. D. Veal, A. Schleife, J. Zúñiga-Pérez, B. Martel, P. H. Jefferson, F. Fuchs, V. Muñoz-Sanjosé, F. Bechstedt, and C. F. McConville, Phys. Rev. B **79**, 205205 (2009).
[18] W. Göpel, J. Pollmann, I. Ivanov, and B. Reihl, Phys. Rev. B **26**, 3144 (1982).
[19] N. Ohashi, Y. Adachi, T. Ohsawa, K. Matsumoto, I. Sakaguchi, H. Haneda, S. Ueda, H. Yoshikawa, and K. Kobayashi, Appl. Phys. Lett. **94**, 122102 (2009).
[20] J. J. Yeh and I. Lindau, At. Data Nucl. Data Tables **32**, 1 (1985).
[21] T. D. Veal, P. D. C. King, P. H. Jefferson, L. F. J. Piper, C. F. McConville, H. Lu, W. J. Schaff, P. A. Anderson, S. M. Durbin, D. Muto, H. Naoi, and Y. Nanishi, Phys. Rev. B **76**, 075313 (2007).